Photocurrent spectroscopy in thin-film insulators: Voltage dependence of the external-circuit current*

D. J. DiMaria† and F. J. Feigl
Materials Research Center and Department of Physics, Lehigh University, Bethlehem, Pennsylvania 18015
(Received 11 July 1973)

An analytical model for trapping-state photodepopulation measurements in conductor–thin-film-insulator–conductor structures is presented. The external-circuit-current dependence on applied voltage is determined, and it is shown that moments of the spatial distribution of trapped charge in the insulator can be extracted from collected-charge versus applied-field characteristic curves. The photodepopulation technique is compared with more widely used differential-capacitance and phtoemission-current techniques.

I. INTRODUCTION

Because of the increasing importance of insulating layers in electronics technology, sensitive and highly discriminatory electrical characterization techniques have been developed for defects in insulating thin films which can become charged by trapping free electrons and holes. Among such techniques are differential capacitance and conductance,[1,2] tunneling,[3] space-charge-limited current,[4] interfacial photoemission,[5] and thermally stimulated current.[6] Several recent investigations have made use of the technique of *optically stimulated trap emptying*,[7] or trap *photodepopulation*, to examine bulk defects in insulating films incorporated between conducting layers in a planar capacitor configuration.[8–13] This technique has been demonstrated to be an extremely sensitive probe, capable of measuring trapped charge densities as low as 10^{-6} C/cm^3, or trapping-center concentrations below the part-per-billion level, in films of total volume 10^{-5} cm^3.

In the present paper, an analytical model for optically stimulated trap-emptying experiments is presented. Consideration of an equivalent circuit for a charged planar capacitor leads to the result that important parameters of the spatial distribution of charge-trapping centers within the insulator can be determined from the variation of the charge collected during photodepopulation as a function of applied field.

II. PHOTODEPOPULATION PROCESS: GENERAL ANALYTICAL MODEL

The basic features of the model for photodepopulation of trapped electrons in insulating films are summarized in Figs. 1–4. Figure 1 exhibits the experimental arrangement used for reported experiments[8–13] on metal-insulator-semiconductor (MIS) systems.[14] Light is incident on the insulating film through the 100-Å-thick semitransparent metal electrode of an MIS capacitor. The insulating film (thickness $L = 10^{-5}$–10^{-3} cm) is grown or deposited on a polished single-crystal semiconductor substrate, and thick (10^{-4} cm) metal contact pads (back and front) are vapor deposited for external-circuit contact. The external circuit consists of an electrometer–Coulombmeter and variable high-precision voltage supply in series. The analysis described below applies to a much more general experimental configuration than the MIS structure of Fig. 1. Any experimental geometry consistent with the circuit of Fig. 4 is appropriate. Figure 4 will be discussed in more detail below. Experimental conditions required for at least one of the examples developed in Sec. IV are (i) the light intensity must be uniform throughout the volume of the insulator, and (ii) the over-all geometry must be that of an ideal planar capacitor, since edge effects or fringing-field effects are not considered. The terms "insulator" and "conductor"

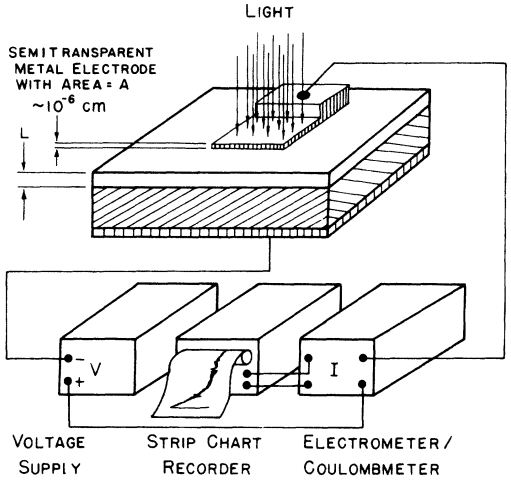

FIG. 1. MIS specimen structure and instrumentation for trap photodepopulation experiments. L is typically 10^{-5}–10^{-3} cm and A is typically 10^{-2}–10^{-1} cm^2.

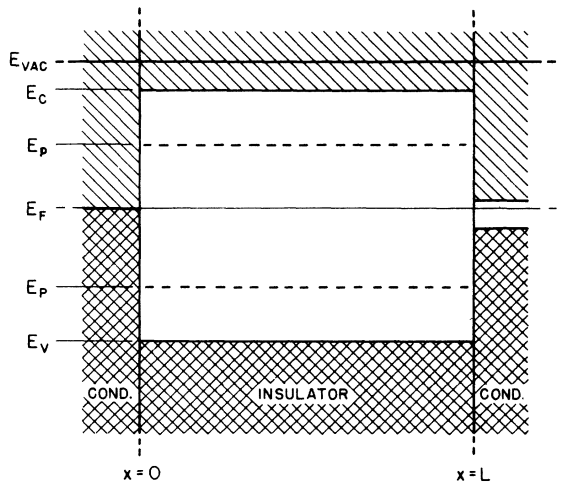

FIG. 2. Idealized energy diagram for MIS specimen. E_V and E_C are valence- and conduction-band edges (or electron and hole mobility edges) for the insulator. Electron-trapping states are located at energies E_p and E_P within the insulator band gap ($E_V<E_P<E_p<E_C$). E_F is the Fermi energy for the MIS system; work-function differences the two conductors are not indicated. "x" is a coordinate normal to the insulator film plane, and, as indicated, $x=0$ corresponds to the metal-insulator interface of an MIS specimen.

are used in a relative sense in this context. The resistivity of the material to be studied must be much greater than that of the electrodes, so that the electric-field boundary conditions developed below are applicable. Clearly, the experiments to be described can also be executed on semiconductors. A final practical requirement is that the transient photodepopulation currents to be described below must be observable above any background dark currents or photoemission currents produced by the illumination.

The basic process of interest in these experiments is photoexcitation of trapped electrons from localized states within the insulator band gap to mobile states within the insulator conduction band (Fig. 2). It is assumed that electrons excited into mobile states are removed from the insulating film under the influence of an accelerating electric field. This is the photodepopulation process. External circuit current during photodepopulation, or the integral thereof, is measured by the electrometer–Coulombmeter and recorded as a function of time.

Figure 2 is an idealized energy diagram for the MIS-capacitor structure. Throughout the present analysis, one-carrier (electron) processes are considered, so that for a given illumination condition (intensity and spectral distribution of the photoexcitation source, magnitude and sign of applied voltage across the insulating film, and time of illumination, t_B) it is presumed that there is some energy E_B above which all traps are emptied and below which no traps are emptied,[15] so that $E_p>E_B>E_P$. The photodepopulation experiment thus begins with some fraction of the trapping states at E_p and E_P occupied, and ends with the trapping states at E_p empty and those at E_P unchanged.[16] The term *optically accessible trapped charge* refers to electrons in states with energy E_p; the term *fixed charge* refers to electrons in states with energy E_P.

In addition to the energy distribution of trapping states, the spatial distribution of trapped charge across the insulating film is also of major interest. Figure 3 illustrates schematically a distribution of charge and electric field across the conductor-insulator-conductor (e.g., MIS) structure. The distributions are presumed to be isotropic and homogeneous in the two spatial dimensions parallel to the plane of the film. A coordinate system is established as indicated in Figs. 2 and 3 (x normal to the film plane, with conductor-insulator interfaces at $x=0$, L). The distinction for trapped

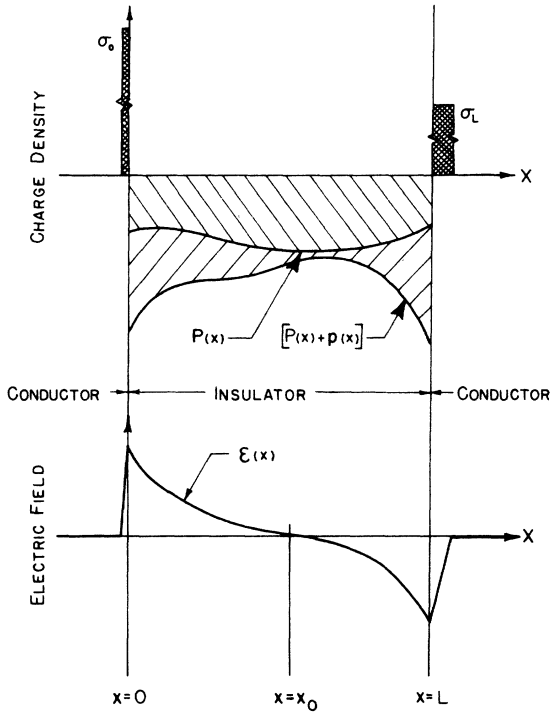

FIG. 3. Charge and field distribution in a planar conductor-insulator-conductor system (x is a coordinate normal to film plane). The situation illustrated corresponds to zero applied field ($V=0$). In practice, the conductors are connected through the external circuitry. The field is related to the charge distributions through Maxwell's equations.

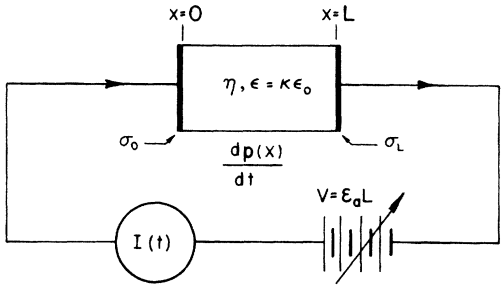

FIG. 4. Idealized parallel-plate-capacitor equivalent circuit proposed for analysis of photodepopulation experiments. Conventional current flow is indicated by arrows. The situation illustrated is *defined* as positive voltage and current.

charge established in connection with energy distributions (Fig. 1) also applied to spatial distributions. $p(x,t)$ represents the spatial charge distribution which can be removed under specific illumination conditions (i.e., charge trapped in states with energy E_p in Fig. 2). $P(x)$ represents charge not removed by this illumination (charge trapped in states with energy E_P in Fig. 2). The field within the insulator at any time is determined by $p(x,t)+P(x)$ and σ_0 or σ_L. σ_0 and σ_L are the interfacial surface-charge densities at $x=0$ and $x=L$, respectively. Thus, the following definitions apply to Figs. 2 and 3: $p(x,t)$ is the volume charge density of optically accessible trapped electronic charge (energy E_p); $P(x)$ is the volume charge density of optically inaccessible trapped electronic charge (energy E_P); $\mathcal{E}(x,t)$ is the electric field at any point x within the insulating film,

$$\epsilon\mathcal{E}(x,t)=\sigma_0(t)+\int_0^x[p(x',t)+P(x')]dx'=-\sigma_L(t)-\int_x^L[p(x',t)+P(x')]dx' \quad .$$

Figure 4 exhibits the equivalent circuit used in the present analysis. It consists of a dielectric-filled capacitor, optical index η and static dielectric constant ϵ, with dielectric charge distributions as indicated in Figs. 2 and 3, and conducting electrodes with surface charge densities σ_0 at $x=0$ and σ_L at $x=L$.[17] This capacitor is in series with a current meter and variable battery. The circuit response time, determined by the insulator capacitance $C=\epsilon/L$ in parallel with connector leakage resistance and the electrometer input resistance, is presumed small compared to response times associated with optical processes. This is a practical restriction that is not necessary for most of the experiments described in Sec. IV. It is required if the detailed time dependence of the external-circuit current is to be studied. The use of such information is described in Sec. IV in connection with Figs. 10 and 11. Throughout the present analysis, it is assumed that photoexcited trapped charge is removed from the insulator and, in particular, that retrapping of release charge is not important.[18] The photodepopulation process is then completely specified by the rate of release of trapped charge, $dp(x,t)/dt$. The equivalent circuit relations governing external circuit response to the photodepopulation process are[19]

$$\sigma_0(t)=\epsilon\mathcal{E}_a-(1-\bar{x}_p/L)\,q(t)-(1-\bar{x}_P/L)\,Q=-\int_0^{x_0(t)}[p(x,t)+P(x)]dx \quad , \tag{1}$$

$$J(t)=\frac{d\sigma_0(t)}{dt}+\int_0^{x_0(t)}\frac{dp(x,t)}{dt}dx \quad . \tag{2}$$

In the above expressions, $\mathcal{E}_a\equiv V/L$, where V is the externally applied voltage across the insulator film and $J(t)$ is the current density averaged over the active-electrode area.[20] The measured external-circuit current $I(t)$ is $J(t)A$, where A is the active electrode area. $x_0(t)$ is the zero-field point (see Fig. 3).

In Secs. III and IV, $J(t)$ will be demonstrated to be a function of the zeroth moment (total charge) and first moment (centroid) of the charge-density distributions defined above. These moments are defined as follows: $q(t)$ is the total optically accessible trapped charge per unit electrode area,

$$q(t)\equiv\int_0^L p(x,t)\,dx \quad ;$$

$\bar{x}_p$ is the centroid of optically accessible trapped charge,

$$\bar{x}_p\equiv[1/q(t)]\int_0^L xp(x,t)\,dx \quad ;$$

Q is the total optically inaccessible trapped charge per unit electrode area,

$$Q\equiv\int_0^L P(x)\,dx \quad ;$$

and $\bar{x}_P$ is the centroid of optically inaccessible trapped charge,

$$\bar{x}_P\equiv(1/Q)\int_0^L xP(x)\,dx \quad .$$

III. PHOTODEPOPULATION EXPERIMENTS: VOLTAGE DEPENDENCE OF EXTERNAL-CIRCUIT RESPONSE

The general result desired is the functional dependence of $J(t)$ on $\mathcal{E}_a$, for all times t such that $0\le t\le t_B$. q, σ_0, and σ_L, $\mathcal{E}(x)$ and x_0, as well as the external-circuit current $J(t)A$ and the trapped charge $p(x,t)$, may be time-varying for $0\le t\le t_B$ (see Figs. 3 and 4). At $t=t_B$, the illumination is terminated and the insulator is in the optically bleached state.[21] At any time t, $x_0(t)$ is the zero-field point within the insulating film, and is thus defined by the condition $\mathcal{E}(x_0,t)=0$.

The analysis of $J(t)$ vs $\mathcal{E}_a$ is most easily accom-

plished by considering two distinct regions of applied field $\mathcal{E}_a$. If at any time t the magnitude of the applied field is sufficiently large, then the zero-field point x_0 cannot be defined. Formally, the zero-field point is then outside the insulator layer, i.e., $x_0 < 0$ or $x_0 > L$. Physically, the electric field $\mathcal{E}(x,t)$ has the same sign, either negative or positive, for all values of x such that $0 \le x \le L$. In this case, with the assumptions discussed above, Eqs. (1) and (2) yield the results

$$J(t) = -\left(1 - \frac{\bar{x}_p}{L}\right)\frac{dq(t)}{dt}\ , \quad x_0(t) = 0 \tag{3a}$$

$$J(t) = +\frac{\bar{x}_p}{L}\frac{dq(t)}{dt}\ , \quad x_0(t) = L\ . \tag{3b}$$

In the above expressions, $dq(t)/dt$ is the net rate of release of trapped charge by photoexcitation.[22] The second region of applied field is defined by the inequality $0 < x_0(t) < L$. In this case, Eqs. (1) and (2) can be combined to yield

$$J(t) = -\frac{1}{q(0)}\frac{dq(t)}{dt}\left[\left(1 - \frac{\bar{x}_p}{L}\right)q(0) - \int_0^{x_0(t)} p(x,0)\,dx\right]\ , \quad 0 < x_0(t) < L \tag{4a}$$

or

$$J(t) = -\frac{1}{q(t)}\frac{dq(t)}{dt}\left[\epsilon\mathcal{E}_a - \left(1 - \frac{\bar{x}_P}{L}\right)Q + \int_0^{x_0(t)} P(x)\,dx\right],\ \ 0 < x_0(t) < L\ . \tag{4b}$$

Again, $dq(t)/dt$ is the net rate of release of trapped charge by the photoexcitation process.[23]

The general solution for the current density is obtained by combining Eqs. (3) and (4):

$$J(t) = -\frac{1}{q(0)}\frac{dq(t)}{dt}\left[\left(1 - \frac{\bar{x}_p}{L}\right)q(0) - \int_0^{x_0(t)} p(x,0)\,dx\right][1 - u(t - t_0)] - \left(1 - \frac{\bar{x}_p}{L}\right)\frac{dq(t)}{dt}[u(t - t_0)] \tag{5a}$$

or

$$J(t) = -\frac{1}{q(t)}\frac{dq(t)}{dt}\left[\epsilon\mathcal{E}_a - \left(1 - \frac{\bar{x}_P}{L}\right)Q + \int_0^{x_0(t)} P(x)\,dx\right][1 - u(t - t_0)] - \left(1 - \frac{\bar{x}_p}{L}\right)\frac{dq(t)}{dt}[u(t - t_0)] \tag{5b}$$

in the region of negative applied voltages as $x_0(t) \to 0$. In the region of positive applied voltages as $x_0(t) \to L$,

$$J(t) = -\frac{1}{q(0)}\frac{dq(t)}{dt}\left[\left(1 - \frac{\bar{x}_p}{L}\right)q(0) - \int_0^{x_0(t)} p(x,0)\,dx\right][1 - u(t - t_L)] + \frac{\bar{x}_p}{L}\frac{dq(t)}{dt}[u(t - t_L)] \tag{6a}$$

or

$$J(t) = -\frac{1}{q(t)}\frac{dq(t)}{dt}\left[\epsilon\mathcal{E}_a - \left(1 - \frac{\bar{x}_P}{L}\right)Q + \int_0^{x_0(t)} P(x)\,dx\right][1 - u(t - t_L)] + \frac{\bar{x}_p}{L}\frac{dq(t)}{dt}[u(t - t_L)]\ . \tag{6b}$$

The two solutions, Eqs. (5) and (6), join when $x_0(t) = \bar{x}_p$. For this situation, the external-circuit current is zero. t_0 and t_L will be defined shortly. In the above expressions, $u(y) = 0$, $y < 0$, and $u(y) = 1$, $y \ge 0$. Equations (5) and (6) apply to the most general experimental situation, for which the zero-field point will initially be at some interior position within the insulating film $[0 < x_0(0) < L]$, so that $V_0 < \mathcal{E}_a L < V_L$, where

$$V_0 = +(1/\epsilon)[(L - \bar{x}_p)q(0) + (L - \bar{x}_P)Q] \tag{7a}$$

and

$$V_L = -(1/\epsilon)[\bar{x}_p\, q(0) + \bar{x}_P\, Q]\ . \tag{7b}$$

At some time t_0 or t_L during the photodepopulation process the zero-field point may be driven to one or the other interface,

$$x_0(t_0) = 0 \Rightarrow +(1/\epsilon L)[(L - \bar{x}_p)\,q(t_0) + (L - \bar{x}_P)\,Q] = \mathcal{E}_a \tag{8a}$$

or

$$x_0(t_L) = L \Rightarrow -(1/\epsilon L)[\bar{x}_p\, q(t_L) + \bar{x}_P\, Q] = \mathcal{E}_a\ . \tag{8b}$$

Equations (8) are defining equations for the quantities t_0 and t_L introduced in Eqs. (5) and (6).

The remainder of the present paper will be concerned with $\mathcal{Q}$-vs-$\mathcal{E}_a$ measurements, where

$$\mathcal{Q}(t_B) = \int_0^{t_B} J(t)\,dt$$

is the net charge transported in the external circuit per unit active-electrode area. General expressions for $\mathcal{Q}(t_B)$ are obtained by integrating Eqs. (5) and (6):

$$\mathcal{Q}(t_B) = \left(1 - \frac{\bar{x}_p}{L}\right)[q(0) - q(t_B)] + \int_0^{t_0} \frac{dq(t)}{dt}\left(\int_0^{x_0(t)} \frac{p(x,0)}{q(0)}\,dx\right)dt$$

$$= \left[\epsilon\mathcal{E}_a - \left(1 - \frac{\bar{x}_P}{L}\right)Q\right]\ln\frac{q(0)}{q(t_0)} + \left(1 - \frac{\bar{x}_p}{L}\right)[q(t_0) - q(t_B)] - \int_0^{t_0} \frac{1}{q(t)}\frac{dq(t)}{dt}\left(\int_0^{x_0(t)} P(x)\,dx\right)dt \tag{9}$$

in the region of negative applied voltages $[x_0(t) \to 0]$, and

$$\mathcal{Q}(t_B) = [q(0) - q(t_L)] - \frac{\bar{x}_p}{L}[q(0) - q(t_B)] + \int_0^{t_L} \frac{dq(t)}{dt}\left(\int_0^{x_0(t)} \frac{p(x,0)}{q(0)}dx\right)dt$$

$$= \left[\epsilon\mathcal{E}_a - \left(1 - \frac{\bar{x}_P}{L}\right)Q\right]\ln\frac{q(0)}{q(t_L)} - \frac{\bar{x}_p}{L}[q(t_L) - q(t_B)] - \int_0^{t_L} \frac{1}{q(t)}\frac{dq(t)}{dt}\left(\int_0^{x_0(t)} P(x)\,dx\right)dt \tag{10}$$

in the region of positive applied voltages $[x_0(t) \to L]$.

A simplified description of the collected-charge–vs–applied-field experiment applies when illumination proceeds to the point that the initial trapped charge has been completely removed from the film. The corresponding analytical limit is $q(t_B) \to 0$ as $t_B \to \infty$, and in this infinite-bleaching-time limit,

$$\mathcal{Q}(\infty) = \left(1 - \frac{\bar{x}_p}{L}\right)q(0) + \int_0^{t_0} \frac{dq(t)}{dt}\left(\int_0^{x_0(t)} \frac{p(x,0)}{q(0)}\,dx\right)dt$$

$$= \left[\epsilon\mathcal{E}_a - \left(1 - \frac{\bar{x}_P}{L}\right)Q\right]\ln\frac{q(0)}{q(t_0)} + \left(1 - \frac{x_p}{L}\right)q(t_0) - \int_0^{t_0} \frac{1}{q(t)}\frac{dq(t)}{dt}\left(\int_0^{x_0(t)} P(x)\,dx\right)dt \tag{11}$$

in the region of negative applied voltages $[x_0(t) \to 0]$, and

$$\mathcal{Q}(\infty) = \left(1 - \frac{x_p}{L}\right)q(0) - q(t_L) + \int_0^{t_L} \frac{dq(t)}{dt}\left(\int_0^{x_0(t)} \frac{p(x,0)}{q(0)}\,dx\right)dt$$

$$= \left[\epsilon\mathcal{E}_a - \left(1 - \frac{x_P}{L}\right)Q\right]\ln\frac{q(0)}{q(t_L)} - \frac{\bar{x}_p}{L}q(t_L) - \int_0^{t_L} \frac{1}{q(t)}\frac{dq(t)}{dt}\left(\int_0^{x_0(t)} P(x)\,dx\right)dt \tag{12}$$

in the region of positive applied voltages $[x_0(t) \to L]$.

IV. PHOTODEPOPULATION EXPERIMENTS: ANALYTICAL AND NUMERICAL EXAMPLES

Figures 5–7 exhibit $\mathcal{Q}$-$\mathcal{E}_a$ response calculated for a number of different charge distributions of the general form

$$P(x) = P_0 e^{-x/\Lambda} \tag{13a}$$

$$p(x,t) = p_0 e^{-x/\Lambda} e^{-t/\tau}\,, \tag{13b}$$

where P_0, p_0, Λ, and τ are adjustable parameters. The three figures correspond to different situations: (i) $P(x)$ and $p(x,t)$ are uniform (Fig. 5); (ii) $P(x)$ varies exponentially from one interface, $p(x,t)$ is uniform (Fig. 6); and (iii) $P(x)$ is uniform, $p(x,t)$ varies exponentially from one interface (Fig. 7). In all cases, $p(x,t)$ is assumed to exhibit an exponential time dependence (consistent with a "monoenergetic" trapping-state distribution depopulated at $h\nu_b > E_C - E_p$, as in Fig. 2). The several curves in each of Figs. 5–7 correspond to different values of P_0 for fixed p_0. Analytical details of the calculations leading to Figs. 5–7 are presented in the Appendix.

The *saturation regions* in the $\mathcal{Q}$-$\mathcal{E}_a$ data are apparent in the diagrams, and the saturation-threshold fields [$\mathcal{E}_a = V_0/L$ and $\mathcal{E}_a = V_L/L$, see Eqs. (7)] are indicated. In these saturation regions $d\mathcal{Q}/d\mathcal{E}_a = 0$. In all cases, the zero and first moments of the spatial distribution of optically accessible charge can be obtained directly from the saturated collected charges:

$$q(0) \equiv \int_0^L p(x,0)\,dx = \mathcal{Q}_0 - \mathcal{Q}_L\,, \tag{14a}$$

$$\frac{\bar{x}_p}{L} \equiv \int_0^L \frac{xp(x,0)}{q(0)}dx = \frac{1}{2}\left(1 - \frac{\mathcal{Q}_0 + \mathcal{Q}_L}{\mathcal{Q}_0 - \mathcal{Q}_L}\right)$$

$$= -\frac{\mathcal{Q}_L}{\mathcal{Q}_0 - \mathcal{Q}_L}\,. \tag{14b}$$

Equations (14) are obtained from Eqs. (11) and (12) in the limits $t_0,\ t_L \to 0$. In Eqs. (14), $\mathcal{Q}_0$ is the saturation collected charge for $\mathcal{E}_a < V_0/L$, and $\mathcal{Q}_L$ is the saturation collected charge for $\mathcal{E}_a > V_L/L$. The zero and first moments of optically inaccessible trapped charge, or fixed charges, can be obtained directly from the saturation-threshold voltages V_0 and V_L:

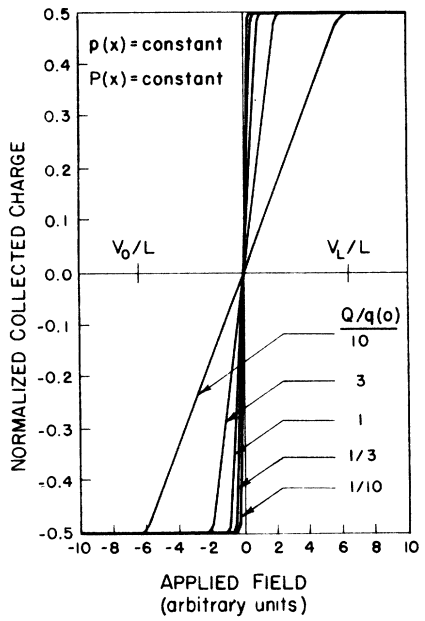

FIG. 5. Normalized collected charge $\mathcal{Q}(\infty)$ vs applied field $\mathcal{E}_a$ for uniform optically accessible charge distribution ($\Lambda \to \infty$) and uniform fixed charge ($\Lambda \to \infty$). Both distributions are negative. The ordinate is collected charge normalized to total optically accessible charge $q(0)$. The several curves correspond to different values of total fixed charge Q for one value of total optically accessible charge $q(0)$. The abscissa scale is arbitrary. For any given $\mathcal{Q}-\mathcal{E}_a$ curve, the quantity $-[Q+q(0)]/\epsilon = (V_L - V_0)/L$ provides suitable field normalization [see Eqs. (7) of text]. The saturation threshold fields V_0/L and V_L/L are indicated for the curve $Q/q(0) = 10$.

$$Q \equiv \int_0^L P(x)\,dx = (\epsilon/L)(V_0 - V_L) - q(0) \quad , \qquad (15a)$$

$$\frac{\bar{x}_p}{L} \equiv \int_0^L \frac{xP(x)}{Q}dx = \frac{\epsilon V_L + \bar{x}_p q(0)}{\epsilon(V_L - V_0) + q(0)L} \quad . \qquad (15b)$$

Equations (15) are obtained from Eqs. (7), with $q(0)$ and $\bar{x}_p$ given by Eqs. (14).

Two limiting cases occur. The first involves an arbitrary spatial variation of optically accessible charge, $p(x,t)$, and no fixed charge in the insulator, i.e., $P(x) = 0$, $0 \le x \le L$, or more generally $q \gg Q$. Figure 8 presents a normalized $\mathcal{Q}$-$\mathcal{E}_a$ response curve applicable to all such cases for both positive and negative applied fields. [The appropriate saturation collected charge $\mathcal{Q}_0$ or $\mathcal{Q}_L$ as determined by Eq. (14) must be used.] The $\mathcal{Q}$-$\mathcal{E}_a$ curve will always pass through the coordinate origin and both saturation threshold points $\mathcal{E}_a = V_0/L$ and $\mathcal{E}_a = V_L/L$ will lie on the dc capacitance locus $\mathcal{Q}_{0,L} = CV_{0,L}$, as indicated in Fig. 8. C is the oxide capacitance per unit area.

The second limiting case is $q \ll Q$. For this situation, it is approximately true that x_0 does not vary with time. Equations (11) or (12) can be differentiated to yield the important result[9]

$$\frac{d\mathcal{Q}(\infty)}{d\mathcal{E}_a} \cong \epsilon \frac{p(x_0, 0)}{P(x_0)} \text{ if } \frac{V_0}{L} < \mathcal{E}_a < \frac{V_L}{L} \quad . \qquad (16)$$

Examination of Figs. 5–7 indicate that this relation is approximately valid[11] for $q < \frac{1}{3}Q$. This is important in situations in which the spatial distribution of fixed charge can be independently determined (See Sec. V). In the particular case in which the optically accessible charge and fixed-charge spatial distributions are covariant [i.e., $p(x,t)/P(x) = K$ = constant, independent of position], Eq. (16) reduces to the linear relation

$$\mathcal{Q}(\infty) = \epsilon K \mathcal{E}_a, \quad K < \tfrac{1}{3} \quad . \qquad (17)$$

Thus, a linear $\mathcal{Q}$-$\mathcal{E}_a$ characteristic curve passing through the coordinate origin will result from arbitrary but identical spatial variations of optically accessible and fixed charge if $q(0) \ll Q$. This situation is graphed in Fig. 9. It must be emphasized that the saturation threshold relations, Eqs. (7), hold in all cases.[24]

It is interesting to examine the time-resolved currents $J(t)$ for the limiting cases just discussed. Figure 10 exhibits J vs t corresponding to the situation $Q = 0$, with $\mathcal{E}_a$ variable (cf. Fig. 8). Figure 11 exhibits similar data corresponding to the situation $p(x,t)/q(t) = P(x)/Q$ = constant, with $q/Q \ll 1$

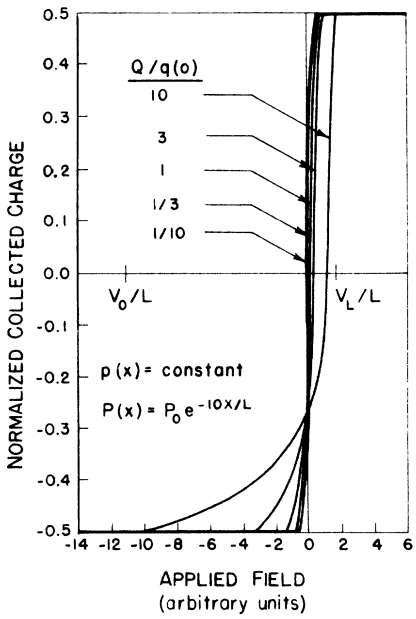

FIG. 6. Normalized collected charge $\mathcal{Q}(\infty)$ vs applied field $\mathcal{E}_a$ for uniform optically accessible charge distribution ($\Lambda \to \infty$) and exponentially varying fixed-charge distribution ($\Lambda = 0.1L$). Both distributions are negative. See caption for Fig. 5 for axis normalization.

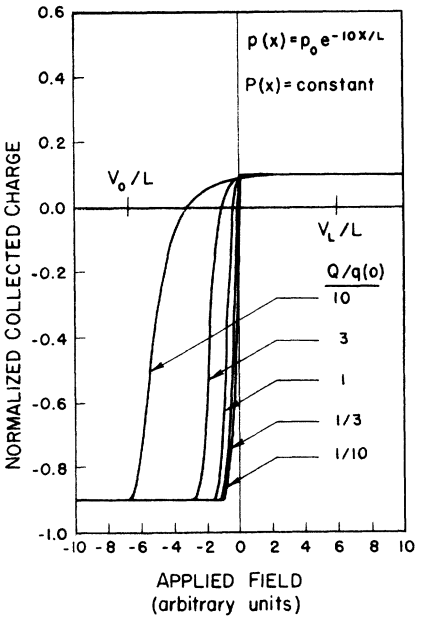

FIG. 7. Normalized collected charge $\mathcal{Q}(\infty)$ vs applied field $\mathcal{E}_a$ for exponentially varying optically accessible charge distribution ($\lambda = 0.1L$) and uniform fixed charge ($\Lambda \to \infty$). Both distributions are negative. See caption for Fig. 5 for axis normalization.

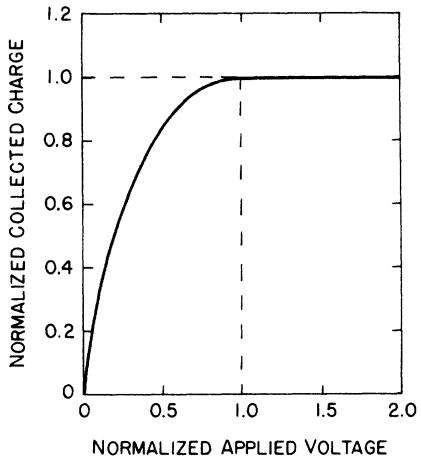

FIG. 8. Normalized collected charge equal to $\mathcal{Q}/\mathcal{Q}_{0,L}$ vs normalized applied voltage equatl to $V/V_{0,L}$ for the case $P(x) = 0$. The saturation charge $\mathcal{Q}_0$ or $\mathcal{Q}_L$ and the corresponding saturation threshold voltage V_0 or V_L are indicated by dash lines. Below the saturation threshold voltage $V_{0,L} \leq \mathcal{Q}_{0,L}/C$,

$$\mathcal{Q} = CV[1 - \ln(V/V_{0,L})],$$

where $C = \epsilon/L$ is the insulator capacitance.

(see Fig. 9). These results are computed through the use of Eqs. (5) and (6) with the assumptions previously stated.

V. DISCUSSION AND CONCLUSIONS

The relationship of saturation-threshold parameters determined from $\mathcal{Q}$-$\mathcal{E}_a$ experiments [Eqs. (14) and (15)] to charge-distribution parameters determined from other experimental techniques for thin-film characterization can be determined. The most important such technique is differential capacitance (C-V). The appropriate $\mathcal{Q}$-$\mathcal{E}_a$ threshold voltage V_L is identical to the C-V flat-band voltage V_{FB} measured at sufficiently high frequency to eliminate fast interface state distortion of the ideal C-V response and corrected for charged-interface-state densities Q_{ss}.[1,2] In both cases, the voltage cited corresponds to that value of applied field at which the zero-field point is driven to the semiconductor-insulator interface.[25] The powerful interface photoemission technique developed by Powell and Berglund can also be compared with $\mathcal{Q}$-$\mathcal{E}_a$ measurements.[5] A lateral displacement of photoemission I-V characteristics along the voltage axis will be induced by any change of net trapped charge in the bulk of the insulator film (by injection or annealing of trapped charge, for example).[5] If this is done without introduction of charge in the immediate region of the emitting interface, no distortion of the I-V characteristic will accompany the lateral displacement.[26] The magnitude of the voltage displacement so measured will equal the change in V_{FB} determined from a high-frequency C-V characteristic, and hence a change in V_0 or V_L determined from a $\mathcal{Q}$-$\mathcal{E}_a$ characteristic. Surface charge

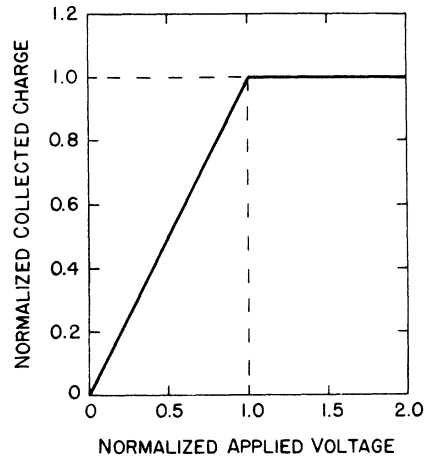

FIG. 9. Normalized collected charge $\mathcal{Q}/\mathcal{Q}_{0,L}$ vs normalized applied voltage $V/V_{0,L}$ for the case $p(x,0)/P(x)$ = constant and $q(0) \ll Q$. The saturation charge $\mathcal{Q}_0$ or $\mathcal{Q}_L$ and the corresponding saturation threshold voltage V_0 or V_L are indicated by dash lines. Below the saturation threshold, the response follows Eq. (17) of the text.

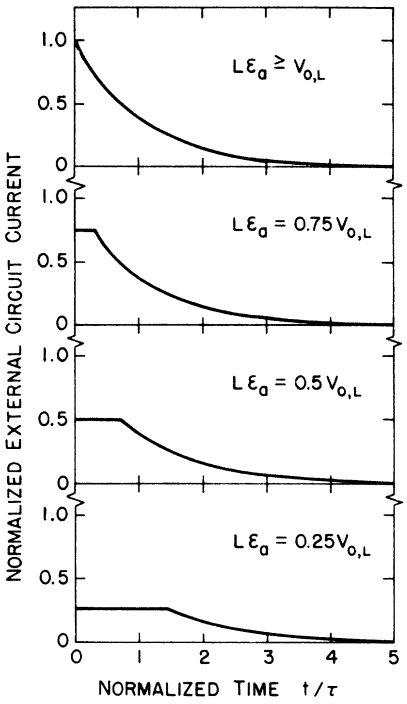

FIG. 10. Photodepopulation current vs time for the case $P(x)=0$. The abscissa is $\tau J/\mathcal{Q}_{0,L}$. The several curves correspond to different values of applied field, as indicated. Single points on the $\mathcal{Q}-V$ curve of Fig. 8 correspond to the integral of the above curves.

and charged interface states produce different effects in photoemission I-V, C-V, and $\mathcal{Q}$-$\mathcal{E}_a$ characteristics, so combinations of these several measurements can be used to separate interfacial and bulk charging effects at both interfaces of a conductor-insulator-conductor system.[5,11,24]

A final point is suggested by the present analysis. The biggest single drawback to application of $\mathcal{Q}$-$\mathcal{E}_a$ characteristic measurements to routine examination of the effect of fabrication, processing, or ambient conditions on insulating films is the extensive time involved. Previous investigators[8-13] have used point-by-point measurements in the infinite-bleaching-time limit discussed in Sec. IV. This can be quite tedious if the characteristic bleaching time τ is of the order of hours. Both high-frequency C-V and photoemission I-V characteristic can be determined in times of the order of minutes using swept-voltage techniques. The photodepopulation experiment could also be executed as a quasistatic swept-voltage measurement. The applicable criterion is that $\tau \gg t_s$, where τ is a characteristic bleaching time for photodepopulation and t_s is the total time required to sweep from some applied voltage less than V_0 to some applied voltage greater than V_L under constant illumination conditions. In this case, the insulator charge distribution would be essentially unchanged throughout the course of the experiment. The instantaneous current would then be determined by Eqs. (5) or (6) with $t=0$:

$$J(\mathcal{E}_a) = +(1/\tau)\left[(1-\bar{x}_p/L)\,q(0) - \int_0^{x_0(\mathcal{E}_a)} p(x,0)\,dx\right] \quad (18a)$$

or

$$J(\mathcal{E}_a) = +(1/\tau)\left[\epsilon\mathcal{E}_a - (1-\bar{x}_p/L)\,Q + \int_0^{x_0(\mathcal{E}_a)} P(x)\,dx\right] , \quad (18b)$$

where it has been assumed that

$$q(t) = q(0)\,e^{-t/\tau} .$$

A comparison of these last relations with Eqs. (11) and (12) shows that all information which can be obtained from point-by-point $\mathcal{Q}$-$\mathcal{E}_a$ characteristic curves can be obtained from voltage swept J-$\mathcal{E}_a$ characteristic curves, if the quasistatic condition $\tau \gg t_s$ can be met. The experiment can be constructed to provide a test of the validity of this approximation: Triangular voltage sweep measure-

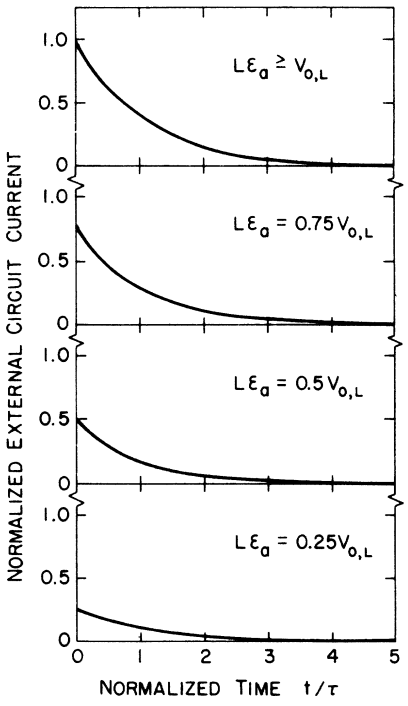

FIG. 11. Photodepopulation current vs time for the case $p(x,0)/P(x)=$ constant and $q(0) \ll Q$. See caption for Fig. 10 for axis normalization. Single points on the $\mathcal{Q}$-V curve of Fig. 9 correspond to the integral of the above curves.

ments should exhibit only slight degenerate hysteresis in J-$\mathcal{E}_a$ characteristics.

In summary, the photodepopulation technique has been demonstrated to be a very powerful complement to other electrical-property measurements on charge trapping in insulating thin films incorporated in MIS or metal-insulator-metal devices. The specificity of this probe to trap distributions at controllable energies is responsible for the two-order-of-magnitude enhancement of sensitivity with respect to C-V or photoemission I-V measurements which are sensitive to *total* bulk trapped charge.[9-12]

ACKNOWLEDGMENTS

Extensive discussions with Professor S. R. Butler and Dr. J. H. Thomas are gratefully acknowledged, as are also conversations with Dr. C. N. Berglund, Dr. R. Williams, and Professor G. J. Borse. The research was supported in part by the Materials Liaison Program at Lehigh University.

APPENDIX

Equations (1), (13a), and (13b) can be combined into the following transcendental equation for $x_0(t)$:

$$0 = \Lambda P_0 (e^{-x_0/\Lambda} - 1) + p_0 \lambda e^{-t/\tau} (e^{-x_0/\lambda} - 1) - \epsilon \mathcal{E}_a + (1 - \bar{x}_p/L) q + (1 - \bar{x}_p/L) Q \quad \text{(A1)}$$

and an expression for collected charge $\mathcal{Q}(\infty)$,

$$\mathcal{Q}(\infty) = -(1 - \bar{x}_p/L)(e^{-(t_0, t_L)/\tau} - 1) q(0) + (p_0 \lambda/\tau) \int_0^{t_0, t_L} e^{-t/\tau} (e^{-x_0/\lambda} - 1)\, dt \quad \begin{cases} + (1 - \bar{x}_p/L) q(0) e^{-t_0/\tau} \\ - (\bar{x}_p/L) q(0) e^{-t_L/\tau} \end{cases} . \quad \text{(A2)}$$

Equation (A2) is used with t_0 or t_L depending on whether $x_0(t)$ is moving towards 0 or L, respectively. From Eq. (A1), it can be shown that

$$t_0 = -\tau \ln \{ [L/q(0)(L - \bar{x}_p)] \times [\epsilon \mathcal{E}_a - (1 - \bar{x}_P/L) Q] \} \quad \text{(A3)}$$

and

$$t_L = -\tau \ln \{ [L/q(0)\bar{x}_p] \times [-\epsilon \mathcal{E}_a - (\bar{x}_P/L) Q] \} . \quad \text{(A4)}$$

A computer program was written to solve the transcendental equation (A1) for $x_0(t)$. Then a numerical integration of (A2) was performed. The results of this program, $\mathcal{Q}(\infty)$ vs $\mathcal{E}_a$, for various values of $Q/q(0)$, Λ, and λ are shown in Figs. 5-7.

*Research supported in part by U. S. Navy Office of Naval Research Contract No. N00014-67A-0370-0004. Based in part on a dissertation submitted by D. J. DiMaria to Lehigh University.

†National Science Foundation Trainee. Present address: IBM Thomas J. Watson Research Center, Yorktown Heights, N.Y. 10598.

[1] A. S. Grove, *Physics and Technology of Semiconductor Devices* (Wiley, New York, 1967), Chaps. 9, 11, and 12.

[2] S. M. Sze, *Physics of Semiconductor Devices* (Wiley-Interscience, New York, 1969), Chaps. 9 and 10.

[3] S. Kar and W. E. Dahlke, Appl. Phys. Lett. 18, 401 (1971); Solid St. Electron. 15, 221 (1972).

[4] M. Lampert and P. Mark, *Current Injection in Solids* (Academic, New York, 1970), Chaps. 1-8.

[5] R. J. Powell and C. N. Berglund, J. Appl. Phys. 42, 4390 (1971); R. J. Powell, IEEE Trans. Nucl. Sci. NS-17, 41 (1970).

[6] J. P. Mitchell, IEEE Trans. Nucl. Sci. NS-15, 154 (1968).

[7] R. H. Bube, *Photoconductivity of Solids* (Wiley, New York, 1960), Chaps. 9 and 10.

[8] R. Williams, Phys. Rev. 140, A569 (1965).

[9] J. H. Thomas and F. J. Feigl, Solid State Commun. 8, 1669 (1970); J. Phys. Chem. Solids 33, 2197 (1972).

[10] J. H. Thomas, J. Appl. Phys. 44, 811 (1973).

[11] D. Mehta, S. R. Butler, and F. J. Feigl, J. Appl. Phys. 43, 4631 (1972); J. Electrochem. Soc. 120, 1707 (1973).

[12] E. Harari and B. S. H. Royce, Appl. Phys. Lett. 22, 106 (1973).

[13] J. D. Brodribb, D. M. Hughes, and T. J. Lewis, Extended Abstracts Electrochemical Society, Abstract No. 104, Fall Meeting (1972) (unpublished); F. C. Aris, D. M. Hughes, T. J. Lewis, Extended Abstracts Electrochemical Society, Abstract No. 129, Fall Meeting (1972) (unpublished).

[14] The analysis applies to any conductor-insulator-conductor structure with appropriate geometry (metal-insulator-metal as well as MIS, for example).

[15] For electron processes, the more general requirement is that traps at energy E_P are not optically active for the specified illumination. The analysis applies also to one-carrier hole processes with appropriate inversion of energy scales (see Lampert and Mark). Free-carrier nonradiative recombination is not considered, however, so the analysis does not apply to two-carrier processes.

[16] The present analysis applies to *photodepopulation* of initially filled trapping states. In previously reported experiments on MIS systems the trapping state distribution was filled by *ultraviolet photoinjection*—capture of electrons introduced into insulator conduction-band states by photoemission from the semiconductor substrate (see Thomas and Feigl; Mehta, Butler, and Feigl; Harari and Royce).

[17] The basic equivalent circuit is similar to that developed

for $C-V$ measurements (see Grove, cited above, and Sze) and interface photoemission (see Powell). As indicated in Figs. 1–3, the convention used for $C-V$ analysis has been adopted: $x=0$ at the metal-insulator interface. This differs from previously used terminology (see Thomas and Feigl).

[18]A. M. Goodman, Phys. Rev. 144, 588 (1966). The assumption of no retrapping is reasonable since the *schubweg* for electrons in MIS structures at fields appropriate to reported photodepopulation experiments is of the order of the insulator thickness.

[19]Equations (1) and (2) are obtained from Poisson's equation and the application of Gauss's law and the continuity equation at the appropriate interface. The photodepopulation process is treated as a quasistationary time-evolving process. These equations can also be written in terms of $\sigma_L(t)$, since $\sigma_0(t)+\sigma_L(t)=-[q(t)+Q]$.

[20]The applied field must be corrected for effective work-function differences between the two conductors, as discussed by Grove and by Sze in connection with $C-V$ measurements. ($V=VA-\varphi_{MS}$ in convertional terminology, where VA is the externally applied voltage.)

[21]The assumptions of an initially filled and terminally empty trapping state distribution is made for convenience only. In general, the photodepopulation experiment proceeds from some initial fractional occupancy of trapping states $f(0)$ to some final fractional occupancy $f(t_B)$, where $0 \leq f(t) \leq 1$.

[22]Equations (6) indicate that at high applied fields, the external-circuit current is proportional to the net photoexcitation rate of trapped electrons. This result is basic to time-resolved and spectrally-resolved photodepopulation experiments described in previous publications (Thomas and Feigl; Mehta, Butler and Feigl).

[23]Alternate forms of important equations, such as (4a) and (4b), are appropriate to different experimental situations, as discussed in Secs. IV and V.

[24]A linear $\mathcal{Q}-\mathcal{E}_a$ characteristic displaced from the origin along the field axis ($\mathcal{Q}=0$ when $\mathcal{E}_a \neq 0$) indicates a large fixed charge very close to an interface ($x=0$ or $x=L$), superimposed on identical optically accessible and fixed-charge distributions.

[25]V_{FB} and $\mathcal{Q}_0$ can be used to determine both the total charge $q(0)$ and the centroid $\bar{x}_p$ (Mehta, Butler, and Feigl; Harari and Royce).

[26]J. R. Brews, J. Appl. Phys. 44, 379 (1973).